arXiv:1409.1096v2 [q-bio.QM] 30 Aug 2016

Diagnostics for assessing the linear noise and moment closure approximations

Colin S. Gillespie and Andrew Golightly

31st August 2016

Solving the chemical master equation exactly is typically not possible, so instead we must rely on simulation based methods. Unfortunately, drawing exact realisations, results in simulating every reaction that occurs. This will preclude the use of exact simulators for models of any realistic size and so approximate algorithms become important. In this paper we describe a general framework for assessing the accuracy of the linear noise and two moment approximations. By constructing an efficient space filling design over the parameter region of interest, we present a number of useful diagnostic tools that aids modellers in assessing whether the approximation is suitable. In particular, we leverage the normality assumption of the linear noise and moment closure approximations.

1 Introduction

Due to advances in experimental techniques, it is now clear that cellular dynamics incorporate a vast array of heterogeneous components. Whilst each component may be relatively simple, combining component systems results in complex, temporal dynamics that are not amenable to simple intuitive understanding.

The recognition of such biological sophistication has lead to the conclusion that complex biological processes cannot be understood through the application of ever-more reductionist experimental programs. Instead, by formulating the system of interest into a mathematical framework, we can begin to combine disparate sources of knowledge. Furthermore, careful mathematical modelling of biological processes has other advantages. For example, Kowald and Kirkwood [1996] highlight possible interactions that would be difficult to observe experimentally. Therefore, a successful analysis of a biological system now requires a complementary wet and dry approach (see Ingalls [2008]).

When modelling biological networks, it is important to incorporate the intrinsic noise of the system. One standard approach is to utilise stochastic kinetic models described using a set of chemical reactions, their associated hazards and an assumption that the system evolves according to a continuous-time Markov jump process (MJP). The transition kernel governing the MJP can be found by constructing and solving Kolmogorov's forward equation, known in this context as the chemical master equation (CME) [Gillespie, 1992]. Unfortunately, the CME is rarely tractable for systems of interest and the vast size of the underlying state space means that numerically computing the solution of the CME is not feasible (see Wilkinson [2012]). While it may not be possible to solve the chemical master equation, it is usually straightforward to obtain exact realisations of the MJP using standard simulation algorithms. The most well known algorithm is the *direct method* developed by Gillespie [1976].

Simulating from the model is not only crucial when building a system, but is also essential for parameter inference, since the observed data likelihood is usually analytically intractable. Exact simulation based approaches to MJP inference typically use data augmentation [Boys et al., 2008] coupled with Markov chain Monte Carlo (MCMC) or particle MCMC [Golightly and Wilkinson, 2011, Owen et al., 2015]. In the simplest implementation of the latter, only forward simulations from the model are required, and the method can be regarded as likelihood-free. Other likelihood-free approaches include the use of approximate Bayesian computation (ABC) schemes [see for example, Beaumont et al., 2002, Sisson et al., 2007, Toni et al., 2009]. These inference schemes typically require many millions of forward simulations and the resulting computational cost may preclude their use when the system size or reaction rates are large. Due to this computational hurdle, a number of approximate simulators have been proposed [for an overview,see Pahle, 2009]. Use of an approximate simulator in this way can be seen as performing exact (simulation-based) inference for the associated approximate model.

Approximate models (and their associated simulators) that ignore the discrete nature of the stochastic kinetic model, but crucially, not stochasticity, include the diffusion approximation [Gillespie, 2000], the linear noise approximation (LNA) [Kurtz, 1970, Elf and Ehrenberg, 2003] and moment closure approaches [van Kampen, 2007, Gillespie, 2009]). Hybrid approaches which treat some species as discrete and others as continuous have been proposed by Salis and Kaznessis [2005] and Sherlock et al. [2014] among others. Moment closure and LNA based approaches are particularly attractive, due to their tractability. For the former, the first two moments of the MJP are combined with an assumption of normality, whereas for the latter, the CME is approximated in a linear way, to give a process with normal transition densities. Unfortunately it is not straightforward to check whether a given approximation technique yields acceptable results since, by definition, the approximate simulator is not exact. For example, if the model contains **any** second-order reactions then the mean population estimate from the linear noise approximation will not be exact (see Golightly and Gillespie [2013] for example). However, the approximation may still be sufficient for model exploration or parameter inference.

Recently, Cao and Petzold [2006] and Jenkinson and Goutsias [2013a] performed a comparison of approximate and exact simulators at specific parameter values. Essen-

tially, each proposed simulating N times from an exact and an approximate algorithm, calculating a distance metric and assessing accuracy by performing a hypothesis test. However, there are two major drawbacks with this test driven approach. First, for many approximate simulators we can analytically prove that the approximate and exact differ, so as N increases we will *always* reject the null hypothesis. Second, in the parameter inference setting we are interested in the performance of the approximate simulator across a range of parameter values, not just at a particular value.

In the related field of computer experiments, complex models are emulated using a faster model; typically a Gaussian process (GP). Since prediction is made using an emulator, it is essential that the emulator accurately represents the system. Bastos and O'Hagan [2009] provide a number of useful diagnostic measures (in the context of Gaussian processes) for assessing simulator quality. Within the context of stochastic kinetic models, both the moment closure and LNA approaches can be seen as GP emulators.

In this paper we present a set of general, principled methods for efficiently assessing the quality of the linear noise and moment closure approximations across a large parameter space based on the techniques found in the computer experiment literature. The diagnostic measures we present are simple to calculate and interpret, providing the practitioner with a useful tool for assessing simulator accuracy. The remainder of this paper is organised as follows. Section 2 briefly reviews stochastic kinetic models and exact simulation techniques before introducing the moment closure and linear noise approximations. In Section 3 we describe efficient methods for exploring the parameter space, and the diagnostic measures which comparisons between simulators are to be based on. The methods are illustrated using three examples of increasing complexity.

2 Stochastic kinetic models

Suppose we have a system of chemical reactions with u chemical species $\{X_1, \ldots, X_u\}$ and v reactions $\{R_1, \ldots, R_v\}$, where reaction R_k, with rate parameter c_k, corresponds to

$$\underline{s}_{k1}X_1 + \ldots + \underline{s}_{ku}X_u \rightarrow \bar{s}_{k1}X_1 + \ldots + \bar{s}_{ku}X_u,$$

with $\underline{s}_{ki}$ and $\bar{s}_{ki}$ the number of molecules of type X_i before and after the reaction R_k, respectively. Let $X_{j,t}$ be the random variable denoting the number of molecules of species X_j at time t and let X_t be the u-vector $X_t = (X_{1,t}, X_{2,t}, \ldots, X_{u,t})'$. Further, let $\underline{s} = (\underline{s}_{ij})$ be a $v \times u$ matrix of the coefficients $\underline{s}_{ij}$ with $\bar{s}$ being defined similarly. Then the $u \times v$ stoichiometry matrix s is defined by

$$s = (\bar{s} - \underline{s})' \,. \tag{1}$$

We denote $x_{i,t}$ to be the number of molecules of species X_i at time t, and let x_t be the u-vector $x_t = (x_{1,t}, x_{2,t}, \ldots, x_{u,t})'$.

The rate of reaction R_k is defined by the rate function $h_k(x_t, c_k)$, where c_k is the reaction rate constant. Hence, the hazard of a type k reaction occurring depends on

the rate constant c_k, as well as the state of the system at time t. This system can be naturally modelled as a Markov jump process, that is, in a small time increment, δt, the probability of reaction R_k occurring in the time interval $(t, t+\delta t]$ is $h_k(x_t, c_i)\delta t$ [Gillespie, 1992]. When a reaction of type k does occur, the system state changes by $\bar{s}_k - \underline{s}_k$. A typical model assumption is that the reactions follow mass action kinetics. This results in a hazard function that takes the form of the rate constant c_k multiplied by a product of binomial coefficients expressing the number of ways in which the reaction can occur.

The transition kernel of the MJP can be found by constructing and solving Kolmogorov's forward equation, known in this context as the chemical master equation (CME). Denote $p(x_t)$ as the probability of being in state x_t and note that we suppress dependence of $p(x_t)$ on the initial state x_0 and the reaction constants $c = (c_1, \ldots, c_v)'$ for simplicity. The CME is given by

$$\frac{d}{dt}p(x_t) = \sum_{k=1}^{v} p(x_t - s_k)h_k(x_t - s_k, c_k) - p(x_t)h_k(x_t, c_k), \tag{2}$$

where $h_k(x_t, c_k)$ is the hazard function for reaction R_k and s_k is the k^{th} column of the matrix s. Once $p(x_t)$ is obtained, a complete characterisation of the system is available. Unfortunately, the CME is only tractable for a handful of cases [see e.g. Gardiner, 1985]. Consequently, for most systems of interest, an analysis via the CME will not be possible.

2.1 Exact simulation

Although the chemical master equation is rarely analytically tractable, it is straightforward to draw exact realisations using a discrete event simulation method. The standard algorithm, developed by Gillespie [1976], for simulating from a stochastic system is the direct method (described in Algorithm 1). Essentially, at each algorithm iteration we select a reaction to occur and update the species levels and clock. However, as the number of reactions or the size of the hazard functions increase, the computational cost increases.

A number of improvements to this algorithm have been proposed. For example, McCollum et al. [2006] dynamically reorder the reactions from most to least likely, to significantly increase the speed of the algorithm. Alternatively Cao et al. [2004] suggest an pilot simulation to optimise the reaction order. Gibson and Bruck [2000] exploit the model structure to avoid unnecessary updates. However, the underlying speed issues still remain for models of reasonable size, necessitating the use of approximate simulation strategies.

2.2 Normal approximations

In what follows, we consider two tractable approximations of $p(x_t)$ that ignore discreteness but not stochasticity. Both approaches assume that the distribution of X_t at a particular time point, t, is normal, so that

$$X_t \sim N(\psi_t(c), \Sigma_t(c)) \tag{3}$$

Algorithm 1: Direct method [Gillespie, 1976]

1: Set $t = 0$ and initialise rate constants $c_1, \ldots, c_v$ and the initial molecule numbers $x_{1,0}, \ldots, x_{u,0}$.
2: Propensities update: update each of the v hazard functions, $h_k(x_t, c_k)$ based on the current state, x_t.
3: Calculate the total hazard, $h_0(x_t, c) = \sum_{k=1}^{v} h_k(x_t, c_k)$.
4: Simulate the time to the next event, $\tau \sim Exp(h_0(x_t, c))$ and set $t = t + \tau$.
5: Simulate the reaction index, j, with probabilities $h_k(x_t, c_k)/h_0(x_t, c), i = 1, \ldots, v$.
6: Update x_t according to reaction j.
7: If simulation time is exceeded, stop, otherwise return to step 2.

where we let the approximate mean and variance $\psi_t(c) = \hat{E}(X_t)$ and $\Sigma_t(c) = \widehat{V}ar(X_t)$ depend explicitly on the rate constants c. Thus the approximate density at a particular time point is

$$\hat{p}(x_t) = \frac{1}{(2\pi)^{u/2}|\Sigma_t(c)|^{1/2}} \exp\left[\frac{1}{2}(x_t - \psi_t(c))' \left[\Sigma_t(c)\right]^{-1}(x_t - \psi_t(c))\right] .$$

It remains that we can choose appropriate forms for $\psi_t(c)$ and $\Sigma_t(c)$. We consider two related approaches, namely, moment closure and the linear noise approximation (LNA). We give a brief, informal description of these techniques in the sequel, and refer the reader to van Kampen [2007] and Wilkinson [2012] for further discussion.

2.2.1 Moment closure

Here, we approximate the moment equations of the system as a set of ordinary differential equations (ODEs). These equations then provide estimates of the mean and variances of individual chemical species.

To extract the moment equations using the moment closure assumption we first define the moment generating function (indexed by θ) as

$$M(\theta; t) = \sum_{x_t} p(x_t) e^{\theta x_t} . \tag{4}$$

The moments, $E[x_t^n]$, where $x_t^n = (x_{1,t}^{n_1}, \ldots, x_{u,t}^{n_u})'$, of the joint probability distribution can be found by taking n^{th} order derivatives of the moment generating function with respect to $\theta = (\theta_1, \ldots, \theta_u)'$. The first moment is the mean and the second moment can be used to obtain the variance.

On multiplying the chemical master equation (2) by $e^{\theta x_t}$ and summing over x_t gives

$$\frac{\partial M(\theta; t)}{\partial t} = \sum_{x_t} e^{\theta x_t} \sum_{k=1}^{v} p(x_t - s_k) h_k(x_t - s_k, c_k) - p(x_t) h_k(x_t, c_k) . \tag{5}$$

The time evolution of the mean concentration of species X_i can be obtained by taking the first derivative of equation (5) with respect to θ_i and then setting θ to zero. Differentiating

equation (5) twice with respect to θ_i yields $E[x_{i,t}^2]$, from which we can obtain the variance. Similarly, differentiating with respect to $\theta_i\theta_j$ gives $E[x_{i,t}\, x_{j,t}]$.

Following this process, we can obtain an ordinary differential equation (ODE) for any moment of interest. However when we have non-linear dynamics, the equation for the i^{th} moment generally depends on the the $(i+1)^{th}$ moment equation, i.e. the ODE for the mean contains a term depending on the second order moment. To circumvent this problem, we need to *close* the system, for example, by assuming an underlying Gaussian distribution. The mean and variance in (3), which we denote by $\psi_t^m(c)$ and $\Sigma_t^m(c)$ in this context, are then easily obtained

Grima [2012] [see also Singh and Hespanha, 2007, Smadbeck and Kaznessis, 2013] shows that increased accuracy of lower-order moment estimation can be obtained by using a higher-order closure scheme. However even though we can estimate higher order moments, it is not clear how these estimates can be routinely utilised. Hence a popular closure choice is to assume normality, resulting in coupled equations for only the mean and variance. This particular closure is also known as the two moment approximation (2MA).

2.2.2 Linear noise approximation

The linear noise approximation can be formed by first constructing the chemical Langevin equation (CLE). In an infinitesimal time interval $(t, t+dt]$, the reaction hazards will remain constant almost surely. This allows us to treat the occurrence of reaction events as the occurrence of events from a Poisson process with independent realisations for each reaction type. Writing dR_t for the v-vector number of reaction events of each type in the time increment, it then follows that $\mathrm{E}(dR_t) = h(X_t, c)dt$ and $\mathrm{Var}(dR_t) = \mathrm{diag}\{h(X_t, c)\}dt$. Using $dX_t = sdR_t$ and matching $\mathrm{E}(dX_t)$ and $\mathrm{Var}(dX_t)$ with the drift and diffusion coefficients of an Itô stochastic differential equation (SDE) gives

$$dX_t = sh(X_t, c)dt + \sqrt{s\mathrm{diag}\{h(X_t, c)\}s'}dW_t \tag{6}$$

where dW_t is the u-dimensional Brownian motion increment. Equation (6) is commonly referred to as the chemical Langevin equation (CLE).

The LNA can now be derived from the CLE as follows. We replace the hazard function in equation (6) with the rescaled form $\Omega f(X_t/\Omega, c)$ where Ω is the cell volume. This results in

$$dX_t = \Omega s f(X_t/\Omega, c)dt + \sqrt{\Omega s\mathrm{diag}\{f(X_t/\Omega, c)\}s'}dW_t\ . \tag{7}$$

Following van Kampen [2007], we write the solution X_t of the CLE as a deterministic process z_t plus a residual stochastic process,

$$X_t = \Omega z_t + \sqrt{\Omega}M_t\ . \tag{8}$$

Then, a Taylor expansion of the rate function around z_t gives

$$f(z_t + M_t/\sqrt{\Omega}, c) = f(z_t, c) + \frac{1}{\sqrt{\Omega}}F_t M_t + O(\Omega^{-1}), \tag{9}$$

where F_t is the $v \times u$ Jacobian matrix with $(i,j)^{\text{th}}$ element $\partial f_i(z_t, c)/\partial z_{j,t}$ and $z_{j,t}$ is the jth component of z_t. Note that we suppress the dependence of F_t on z_t and c for simplicity. Substituting (8) and (9) into equation (7) and collecting terms of $O(1)$ and $O(1/\sqrt{\Omega})$ give the ODE satisfied by z_t, and SDE satisfied by M_t respectively, as

$$dz_t = s\, f(z_t, c)dt, \tag{10}$$

$$dM_t = s\, F_t M_t dt + \sqrt{s\,\mathrm{diag}\{f(z_t, c)\}s'}\, dW_t. \tag{11}$$

Equations (8), (10) and (11) give the linear noise approximation of the CLE and in turn, an approximation of the Markov jump process model.

For fixed or Gaussian initial conditions, the stochastic differential equation in (11) can be solved explicitly to give $(M_t|\, c) \sim N(m_t, V_t)$ where m_t and V_t satisfy the coupled deterministic system of ordinary differential equations

$$\frac{dm_t}{dt} = sF_t m_t, \tag{12}$$

$$\frac{dV_t}{dt} = V_t F_t' s' + s\mathrm{diag}\{h(z_t, c)\}s' + s' F_t V_t\ . \tag{13}$$

Hence, the approximating distribution of X_t is as (3) with

$$\psi_t^l(c) = \Omega z_t + \sqrt{\Omega} m_t, \qquad \Sigma_t^l(c) = \Omega V_t\ . \tag{14}$$

In situations where the ODE satisfied by z_t is initialised with $z_0 = x_0$ so that $m_0 = 0$, we see that $m_t = 0$ for all t and $\psi_t^l(c) = \Omega z_t$. Note further that Ω plays no role in the evolution equations (10) and (13). Therefore, in the examples in section 4, we assume a unit volume ($\Omega = 1$) for simplicity.

3 Diagnostic tools

When model building, we usually want to investigate many different parameter combinations. Similarly when inferring parameters, the data available is usually limited and prior information on the plausible parameter values is sparse. Therefore, parameter inference and model exploration usually follows a combination of parameter scans, and/or exploring the parameter space using efficient inference algorithms.

Since the parameter space to search will be large, it would be computationally unfeasible to numerically assess the approximate simulator at all values. In particular, since an approximate algorithm is being utilised, this implies that simulating exact realisations may be computationally intensive. Thus the parameter space must be explored efficiently.

One approach to explore the parameter space is random sampling, that is, we sample uniformly in the parameter space. However, McKay et al. [1979] showed that Latin hypercube sampling (LHS) gave a significant improvement over simple random sampling when exploring large spaces. Morris and Mitchell [1995] improved the original LHS design with the maximin design, in which the distance between points in the hypercube

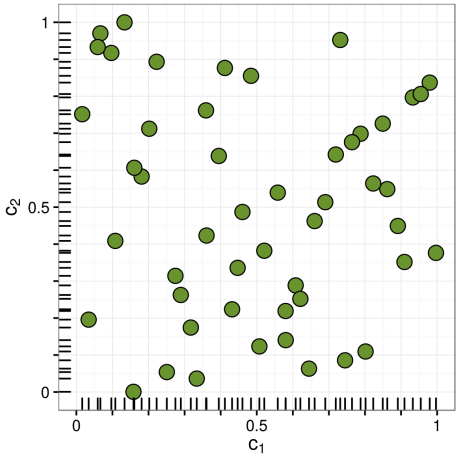

Figure 1: A two–dimensional Latin hypercube design, with $n_d = 50$ points.

is maximised. Moreover, Latin hypercube sampling of the parameter space lends itself to an embarrassingly parallel mode of computation. Naturally, in scenarios that do not require a covering of the whole parameter space, other methods may be preferred. For example, if performing Bayesian inference via Markov chain Monte Carlo (MCMC) and focusing on regions of high posterior density, then we may choose to use the output of the MCMC scheme.

Figure 1 illustrates a two–dimensional design over parameters (c_1, c_2), with $n_d = 50$ points. We denote the n_d points in the Latin hypercube as

$$\gamma = (\gamma_1, \ldots, \gamma_{n_d}) \, .$$

Hence, each point γ_i is a length-v (column) vector of parameter values, that is $\gamma_i = (c_{1,i}, \ldots, c_{v,i})'$. A feature of these space filling designs, is that the marginal parameter distributions have a uniform distribution, thereby giving good coverage in each dimension.

Our general strategy is to compare the moment closure/linear noise approximation to a single realisation simulated exactly (using Algorithm 1) from the Markov jump process, at each of the n_d points in the design. We refer to Algorithm 1 as the exact simulator. For each design point γ_i let $\mathbf{x}^*(\gamma_i) = (x_1^*(\gamma_i), \ldots, x_u^*(\gamma_i))'$ denote a single realisation from the exact simulator at a particular time point, with dependence on time, and the initial conditions used to produce the realisation, suppressed for ease of notation. In the following sections, we describe simple diagnostics that can be assessed by comparing the observed diagnostic at $\mathbf{x}^*(\gamma_i)$ with the reference distribution of the diagnostic induced by the approximations described in (2.2).

3.1 Individual prediction errors

One way of assessing the accuracy of a Gaussian based approximation is to calculate individual prediction errors. These are obtained by calculating the difference between

the exact simulator and the mean of the linear noise (or two moment) approximation, that is

$$e_{i,j} = x_j^*(\gamma_i) - \psi_j(\gamma_i) \tag{15}$$

for each point $i = 1, \ldots, n_d$ and species $j = 1, \ldots, u$. Note that $\psi_j(\gamma_i)$ denotes the jth component of the mean in (3) after omitting dependency on time t. Plainly, a more appropriate quantity to work with is the standardised prediction error

$$e_{i,j}^* = \frac{x_j^*(\gamma_i) - \psi_j(\gamma_i)}{\sqrt{\Sigma_{jj}(\gamma_i)}} \, . \tag{16}$$

If $\mathbf{x}^*(\gamma_i)$ is replaced with a draw from either the two moment or linear noise approximation, then the standard prediction errors can be seen as draws from a standard normal distribution. Hence, large standardised individual errors, with absolute values larger than say two, indicate a potential discrepancy between the exact and approximate simulators. Of course, single, isolated values are possible, and so further investigation can be performed by obtaining more simulator runs in the parameter vicinity.

Since the reference distribution of the standardised prediction errors is normal, we can use other standard techniques for assessing the modelling assumptions that underpin both approximate simulators. For example, quantile-quantile (q-q) plots provide a natural graphical diagnostic for assessing normality, with a reasonable fit indicated by points close to a 45-degree line through the origin. We may expect the output of the exact simulator to be heavier tailed than a Gaussian, in which case points in the q-q plot will cluster around a line with a slope greater than one. Plotting errors against parameter values may also be useful in identifying regions of parameter space that exhibit large discrepancies.

We note that at each point on the Latin hypercube, it is possible to draw n_{ex} realisations from an exact simulator (giving a total of $N = n_d \times n_{ex}$ exact simulations), and use a formal hypothesis test in the spirit of Jenkinson and Goutsias [2013b]. However, there are a number of potential drawbacks with this approach. First, the computational cost may be prohibitively large. For a fixed computational budget of N simulations, either n_{ex} would be prohibitively small, which would adversely affect the power of the test, or we would reduce n_d and not explore the parameter space. Second, for both the LNA and 2MA schemes, if the model contains a second order reaction, we can prove analytically that the mean and variance are not equal to the true value, so a hypothesis test is not needed. Furthermore, any non-significant test must be spurious. Third, the normal assumption is also clearly incorrect since the state space is discrete. Therefore, we focus on an assessment of whether the approximation is "good enough" over a large parameter space.

3.2 Interval diagnostic

Another straightforward method for assessing fit is to construct a $100\alpha\%$ confidence interval for $x_j^*(\gamma_i)$ using the mean $\psi(\cdot)$ and variance $\Sigma(\cdot)$ associated with the approximate simulator under assessment. We denote a particular confidence interval at design point

i, for species j, as $CI_{i,j}(\alpha)$. The proportion of simulated values that land within the confidence region is given by

$$D_j^{CI} = \frac{1}{n_d}\sum_{i=1}^{n_d} 1[x_j^*(\gamma_i) \in CI_{i,j}(\alpha)], \tag{17}$$

where $1[\cdot]$ is the indicator function. We can assess fit as the value of D_j^{CI} should be approximately equal to α. Additionally, plotting the confidence regions against parameter values can highlight any particular systematic deviations.

3.3 LNA vs 2MA

Recently Grima [2012] explored the link between the two moment and linear noise approximations. Essentially, the two approximations are very similar, except that the mean equations in the LNA do not depend on the covariances. This would suggest that if the two approximations gave appreciably different estimates for the first two moments, further investigation is required.

We define the standardised difference between the two approximations as

$$D_j^{LM}(\gamma_i) = \frac{\psi_j^l(\gamma_i) - \psi_j^m(\gamma_i)}{\sqrt{\Sigma_{jj}^l(\gamma_i)}}\,. \tag{18}$$

Note again that for notational convenience, the time subscript t has been omitted from the expression. Large differences of D_j^{LM} should be carefully investigated. This diagnostic measure has the advantage of avoiding (possibly expensive) exact simulation. However, when the two approximations give similar results, it does not necessarily follow that both approximations are correct. For example, Schnoerr et al. [2014] highlighted an oscillating system where the LNA and 2MA schemes were in agreement, but were significantly different from the solution to the underlying chemical master equation.

4 Examples

Here, we demonstrate the diagnostic tools in three examples. Diagnostics based on the linear noise approximation are constructed for two reaction networks that are known to exhibit interesting non-linear dynamics. In the final example, we consider the prokaryotic auto regulatory gene network analysed by Golightly and Wilkinson [2008] and Milner et al. [2013]. We focus on the moment closure approximation and construct diagnostics to assess approximate simulator fit both *a priori* and *a posteriori*. Interactive versions of all graphics can be found at

https://bookdown.org/csgillespie/diagnostics/

4.1 Schlögl system

The Schlögl model is a well known test system that exhibits bi-modal and non-linear characteristics at certain parameter combinations. The system contains four reactions

$$\begin{array}{llll} R_1\colon & 2X_1 + X_2 \xrightarrow{c_1} 3X_1 & R_2\colon & 3X_1 \xrightarrow{c_2} 2X_1 + X_2 \\ R_3\colon & X_3 \xrightarrow{c_3} X_1 & R_4\colon & X_1 \xrightarrow{c_4} X_3 \end{array}$$

describing the evolution of three chemical species, X_1, X_2, and X_3 and assumes mass action kinetics. In this example, we concentrate on species X_1. Where the distribution of X_1 is bi-modal, the linear noise approximation would clearly be inappropriate. However for large models, it isn't necessary clear if (or where) a system would have bi-modal regions. Hence, the purpose of this example is to illustrate how problematic regions may be detected.

The parameters $(c_1, c_2)'$ were fixed at $(3 \times 10^{-7}, 10^{-4})'$ and the initial conditions assumed constant at

$$x_0 = (250, 10^5, 2 \times 10^5)' \, .$$

Suppose that interest lies in the accuracy of the linear noise approximation at time-point $t = 5$. Further, consider a parameter space defined by the regions $c_3 = (10^{-4}, 10^{-2})$ and $c_4 = (10^{-2}, 10)$ (on the $\log_{10}$ scale). Figure 2a shows the region in parameter space that leads to a bi-modal distribution of X_1. The plot was obtained by finely discretising the parameter space (to give a 1000×1000 grid) and calculating the absolute prediction error (on the $\log_{10}$ scale) at each parameter value. For systems of realistic size and complexity, this approach will be computationally prohibitive.

We therefore generated a Latin hypercube with $n_d = 10,000$ points. The two dimensional design space is given in Figure 2a. The standardised prediction errors plotted against parameter c_4 are shown in Figure 2b. The locally smoothed mean value (shown in blue), is close to zero. However there are several large errors, in particular, $e^*_{8684} \simeq 194$. This large error was further investigated using fifty realisations from the exact simulator with the parameter values set at γ_{8684} (see Figure 2d). The LNA mean solution is also shown in red. It is clear that at this particular choice of parameter values, the Schlögl system has a bi-modal distribution and the LNA is inappropriate in this region of parameter space. Therefore, with relatively few design points, we are able to detect regions of parameter space that lead to significant discrepancies between the exact and approximate simulators. Naturally, care must be taken in the choice of n_d and this will typically be dictated by computational budget. We find that for this example, reducing n_d to 1000 results in only a single value in the Latin hypercube design with an absolute prediction error greater than 2.

As discussed in section 3.1, rather than generate a single exact simulation at each of the n_d points, we could simulate N times, where $N = n_d \times n_{ex}$, to give n_{ex} replicates at each of the design points, allowing comparison of the simulator output via a formal hypothesis test. This is similar to the example in Jenkinson and Goutsias [2013b], where the authors set $n_{ex} = 350$. We note that a computational budget allowing $N = 10,000$ would result in only 30 points in the hypercube being assessed. It is highly unlikely, in this case, that the region of bi-modality would be detected.

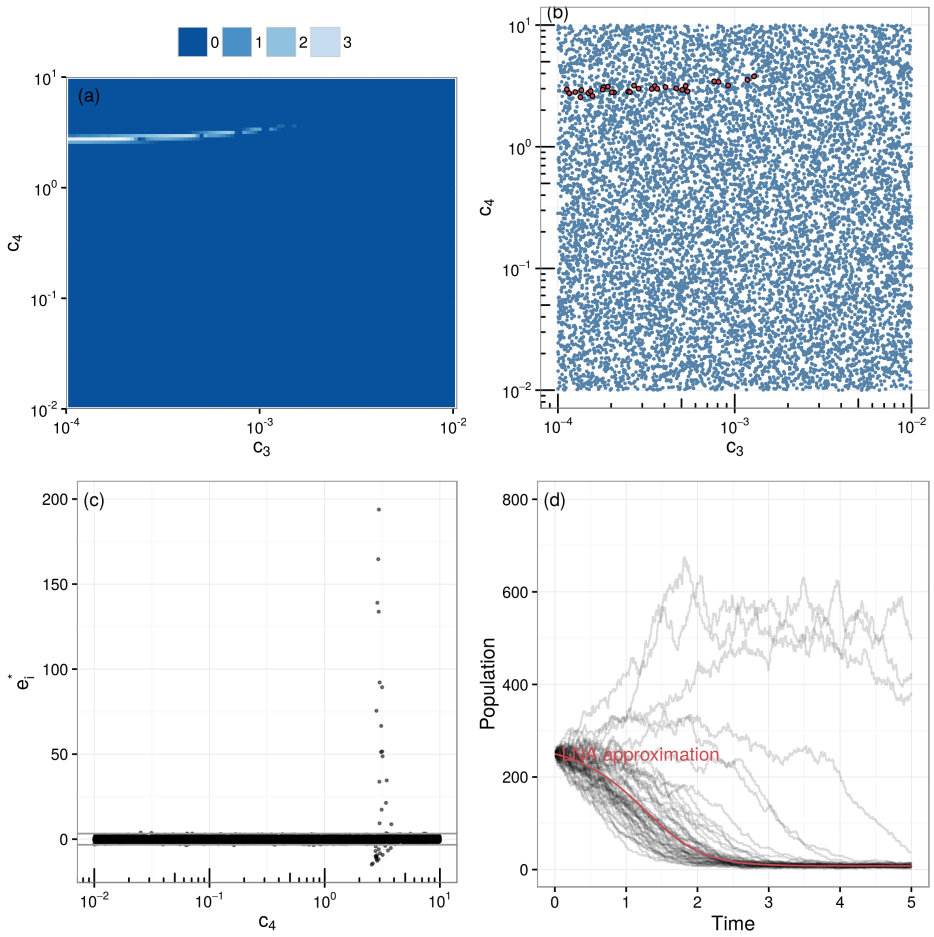

Figure 2: Model diagnostics for the Schlögl system. (a) Image plot highlighting the bi-modality region for the Schlögl system. (b) Latin hypercube design (on the $\log_{10}$ scale), with $n_d = 10,000$. The largest 30 errors are shown in red. (c) Standardised prediction errors, with 95% and 99.9% regions indicated by grey lines. (d) Fifty stochastic simulations, where $c = (3\times10^{-7}, 10^{-4}, 0.00011, 2.955)$ (the parameter values associated with the largest prediction error). The mean of the linear noise approximation is shown in red.

4.2 Lotka-Volterra model

The predator prey system developed by Lotka [1925] and Volterra [1926], describes the time evolution of two species, X_1 and X_2. This system has two species and three reactions

$$R_1\colon\ X_1 \xrightarrow{c_1} 2X_1 \qquad R_2\colon\ X_1 + X_2 \xrightarrow{c_2} 2X_2$$
$$R_3\colon\ X_2 \xrightarrow{c_3} \emptyset\ .$$

Although relatively simple, this system exhibits interesting auto regulatory behaviour and has been used numerous times to test inference algorithms; see, for example, Boys

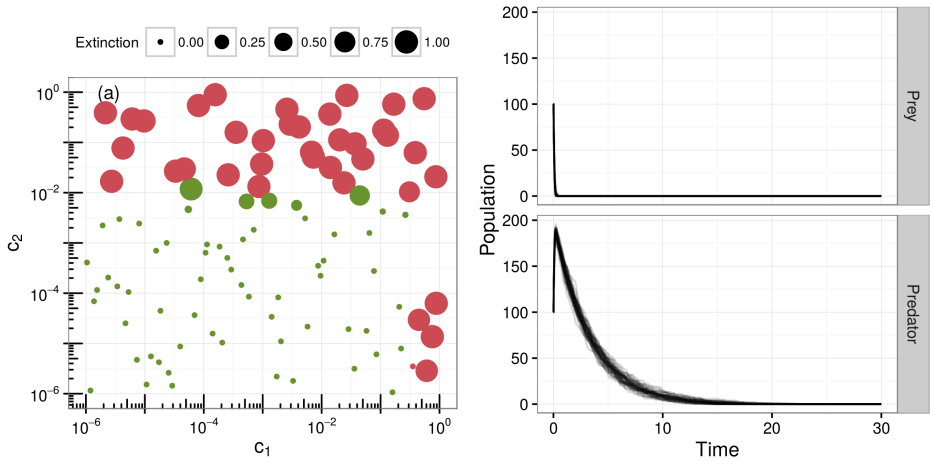

Figure 3: Lotka-Volterra predator prey system. All simulations used initial conditions $x_0 = (100, 100)'$. (a) Latin hypercube design (with $n_d = 100$) on the $\log_{10}$ scale. At each point on the hypercube the D^{LM} diagnostic was calculated. Values where $|D^{LM}_{i,2}| > 5$ are shown as red circles. The radius of each circle is proportional to the probability of prey extinction by time 30. (b) Fifty stochastic simulations with parameter values $c = (10^{-4}, 0.1, 0.3)'$.

et al. [2008], Opper and Sanguinetti [2008], White et al. [2013]. In particular, the linear noise and two moment approximations have been used for parameter inference [Milner et al., 2013, Golightly et al., 2015].

To assess the linear noise approximation, we generated $n_d = 100$ points from a two-dimensional Latin hypercube, over the regions $c_1 = (10^{-6}, 10^0)$ and $c_2 = (10^{-6}, 10^0)$ on the $\log_{10}$ scale. These regions correspond to an inference situation where we are using vague priors. We set $c_3 = 0.3$ and used initial conditions $x_0 = (100, 100)'$ with a maximum simulation time of $t = 30$. Figure 3a shows the Latin hypercube design. The diagnostic of Section 3.3 was computed at each design point. Values where $|D^{LM}_{i,2}| > 5$ are shown as red circles in Figure 3. The radius of each circle is proportional to the probability of prey extinction by time 30. It is clear that for large values of c_1 or c_2, the LNA and 2MA approximations disagree. Moreover, we see that these points coincide with a high probability of prey extinction by time 30 (see also Figure 3b, showing fifty realisations from the exact simulator at a typical discrepant parameter value). This result is perhaps unsurprising given the time-course behaviour of the Markov jump process representation of the Lotka-Volterra system. The system eventually reaches one of two states: if X_1 dies out then the system will run to $(0, 0)$ (reactions 1 and 2 will never again occur). If X_2 dies out the system will go towards $(\infty, 0)$ (reactions 2 and 3 will never again occur). The LNA fails to capture this behaviour. For example, the LNA mean is a perfectly repeating oscillation, carrying on indefinitely. As expected, increasing t leads to a higher proportion of the parameter space with significantly large prediction errors (results not reported).

4.3 Prokaryotic auto regulatory gene network

A more realistic example is the prokaryotic auto regulation system. This larger model contains six species and twelve reactions. In this network a protein I coded for by a gene i represses its own transcription and also the transcription of another gene g by binding to a regulatory region upstream of the gene. This is described by the reactions

$$R_1 \colon I + i \to I \cdot i, \qquad R_2 \colon I \cdot i \to I + i,$$
$$R_3 \colon I + g \to I \cdot g, \qquad R_4 \colon I \cdot g \to I + g.$$

The transcription of i and g and the translation of mRNA r_i and r_g are represented by

$$R_5 \colon i \to i + r_i, \qquad R_6 \colon r_i \to r_i + I,$$
$$R_7 \colon g \to g + r_g, \qquad R_8 \colon r_g \to r_g + G.$$

We also have mRNA degradation

$$R_9 \colon r_i \to \emptyset, \qquad R_{10} \colon r_g \to \emptyset,$$

and protein degradation

$$R_{11} \colon I \to \emptyset, \qquad R_{12} \colon G \to \emptyset.$$

Each reaction i has a stochastic rate constant c_i. There are two conservation laws in the model

$$I \cdot i + i = K_1, \qquad I \cdot g + g = K_2,$$

where K_1 and K_2 are conservation constants. If K_1 and K_2 are known, then we can simplify the model using the conservation laws to remove $I \cdot i$ and $I \cdot g$. This simplification reduces the model to six species

$$x = (I, G, i, g, r_i, r_g)' .$$

The reaction hazards for R_1 and R_2 are $h_1(x, c_1) = c_1 I i$ and $h_2(x, c_2) = c_2 I \cdot i = c_2(K_1 - i)$ respectively. Hazards for R_3 and R_4 are calculated similarly. The remaining hazards are for first order reactions.

This model has been used to test parameter inference schemes by Golightly and Wilkinson [2008] and Milner et al. [2013]. In this example, we will explore the moment closure approach used by Milner et al. [2013].

The stochastic realisation that Milner et al. [2013] based their parameter inference on is given in Figure 4. Many of the chemical species have population sizes less than twenty. However, the population of species G has a population greater than $65,000$. Hence, exact simulations based on parameter values consistent with the data in Figure 4 are computationally expensive. This prohibits the use of inference algorithms based on exact simulation.

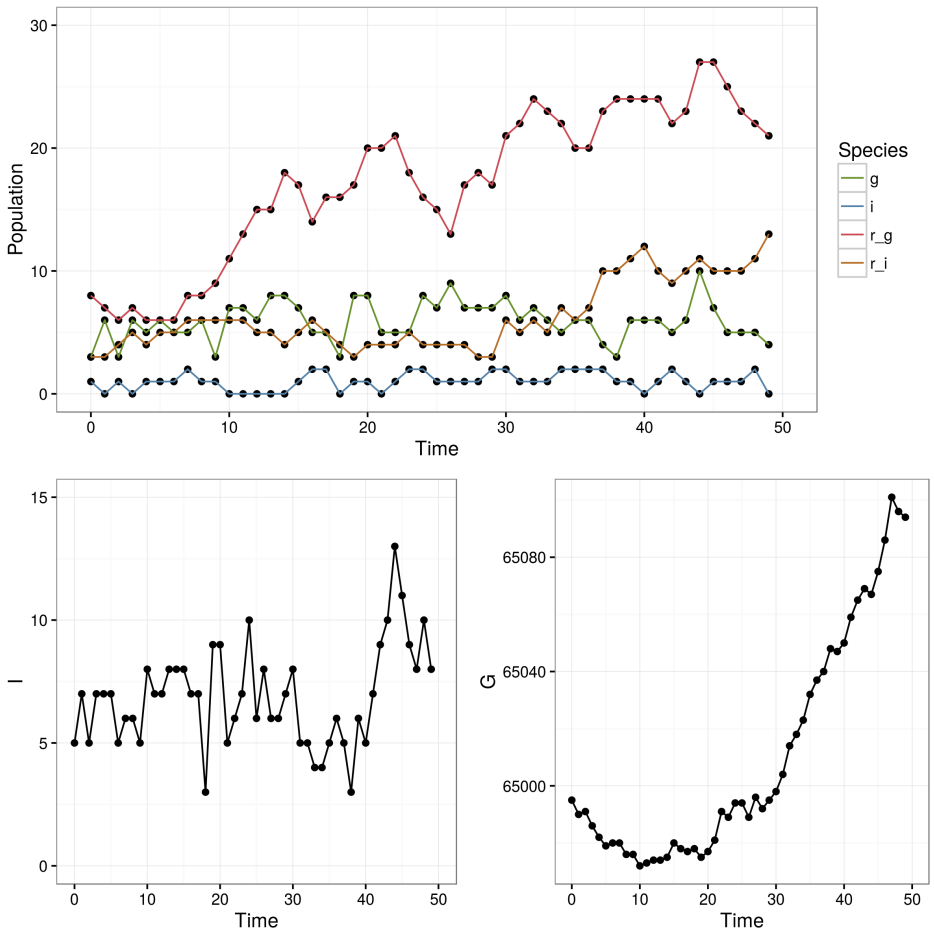

Figure 4: A single stochastic realisation from the prokaryotic auto regulatory gene network. This realisation was observed at times $t = 0, 1, \ldots, 49$.

4.3.1 Inference set-up

We use a data set of fifty observations at (unit) discrete time points of the simulated process (see Figure 4 for the trace of the realisation). The true parameter values for $(c_1, c_2, \ldots, c_{12})$ that produced the data set were $(0.08, 0.82, 0.09, 0.9, 0.75, 0.05, 0.35, 0.5, 0.1, 0.1, 0.05, 0.0001)$. It is worth noting that gene i has at most two copies and only takes values 0, 1 or 2.

Only vague prior knowledge was assumed about parameter values, with Uniform $U(-5, 1)$ priors for each $\log(c_i)$ for $i = 1, \ldots, 12$ and $U(-12, -6)$ on $\log(c_{12})$. The values of K_1 and K_2 were assumed known and set at two and ten respectively.

4.3.2 Prior investigation

An $n_d = 10,000$ point twelve dimensional Latin hypercube was created on the log space over the parameter prior regions. At each point on the hypercube, a time point from

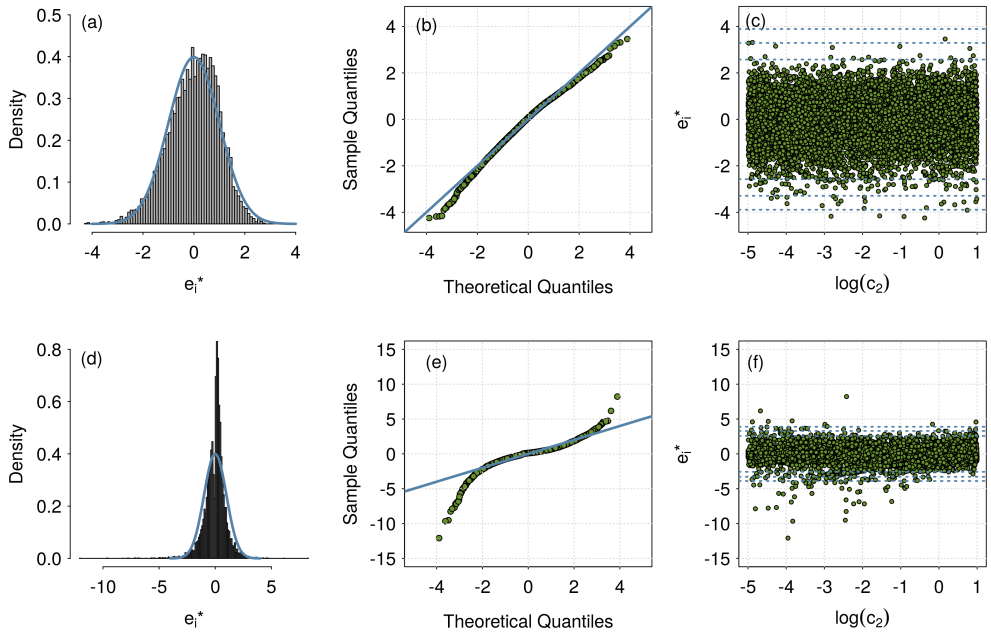

Figure 5: Predictive error plots for `I` (top row) and `i` (bottom row) based on the prior distribution. A total of $n_d = 10,000$ points were sampled from a thirteen dimensional Latin hypercube (twelve parameters plus the time dimensional). The blue lines on figures (a), (b), (d) and (e) represent the standard normal distribution. The dashed lines in figures (c) and (f) represent the 99%, 99.9% and 99.99% regions in the standard normal distribution.

the realisation in Figure 4 was selected to initialise the exact simulator and the moment closure approximation. Each simulator was then run for a single time point and the standardised prediction error was calculated.

Figure 5 (a)–(c) gives the diagnostic plots for species `I`. Although the population levels of I are relatively small, the population size varies between 3 and 13, the associated diagnostic plots still look reasonable. The diagnostic plots for species i are given in Figure 5 (d)–(f). This species only takes values 0, 1, and 2. As would be expected, the diagnostic plots show clear deviations from the normality assumptions. In particular, when $c_2 << 0.1$, we obtain a number of very large standardised prediction errors. As with the Schlögl system, it would be advisable to investigate these problematic points more carefully. We note that for the data set in Figure 4, the marginal posterior density for c_2 has negligible mass in this region of parameter space (the true value of c_2 is 0.82).

4.3.3 Posterior investigation

A further investigation of the appropriateness of the moment approximation can be made *a posteriori*. Since the parameters in the posterior distribution were in some cases highly correlated, we sampled $n_d = 10,000$ points from this posterior.

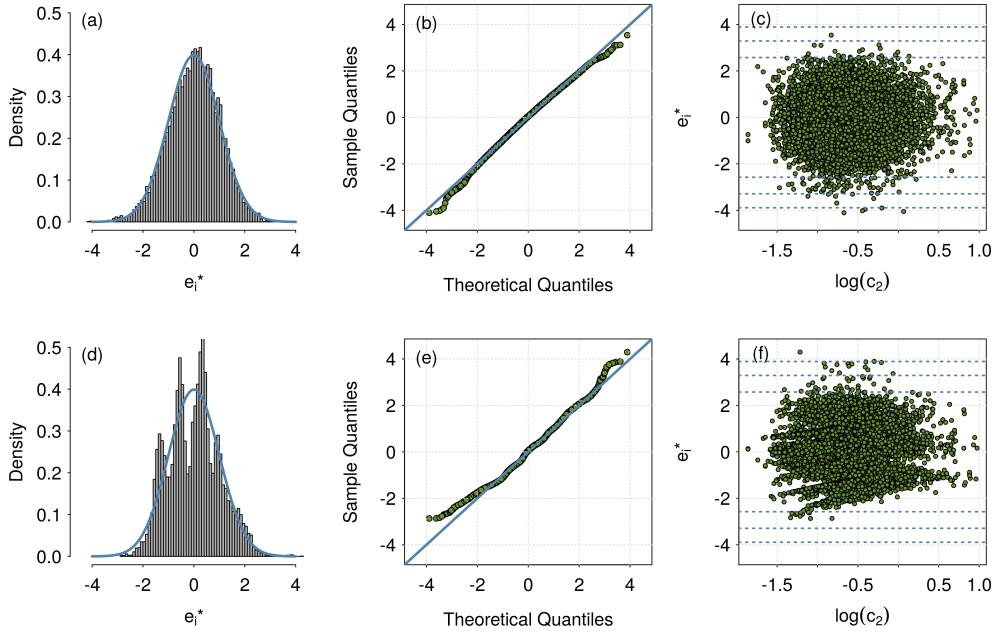

Figure 6: Predictive error plots for `I` (top row) and `i` (bottom row), based on the posterior distribution. A total of $n_d = 10,000$ points were sampled from the posterior distribution. The blue lines on figures (a), (b), (d) and (e) represent the standard normal distribution. The dashed lines in figures (c) and (f) represent the 99%, 99.9% and 99.99% regions in the standard normal distribution.

Again, the diagnostic plots for species I (Figure 6 (a)–(c)) suggest that the normality assumption and the accuracy of the mean and variances of the moment closure approximation appear reasonable. The diagnostic plots for low level species i have substantially improved (see Figure 6 (d)–(e)), although we observe extreme standardised errors in Figure 6 (f). Of course, since i can only take values 0, 1, and 2, the prediction errors are not normally distributed (see Figure 6 (d)). Although the moment closure approach fails to adequately match the Markov jump process in all regions of parameter space *a priori*, in regions of high posterior density, it does appear to provide a satisfactory alternative.

5 Discussion

Analysing stochastic kinetic models of realistic size and complexity is a challenging problem. For example, whilst it is possible, in principle, to perform exact (simulation-based) inference for the Markov jump process (MJP) representation [Boys et al., 2008, Golightly and Wilkinson, 2011, Owen et al., 2015], existing approaches are computationally intensive and have ostensibly focused on toy examples with relatively few numbers of species

and reactions. Replacing the exact MJP simulator with a cheap approximation and using this for model exploration/inference is an appealing alternative approach. Gaussian approximations that ignore discreteness but not stochasticity, such as the linear noise approximation (LNA) and moment closure approaches considered here, are particularly attractive due to their tractability. While this assumption can make inference easier, it is essential to assess the appropriateness of the Gaussian approximation. It is apparent from the literature that such an assessment rarely takes place.

In this paper we have presented a general, easy-to-use, framework that allows modellers to determine whether a given Gaussian approximation is suitable for their model. Following the approach of Bastos and O'Hagan [2009], we have examined simple numerical diagnostics, by constructing appropriate functions of the exact simulator output. Comparing observed values of the diagnostic (for a particular parameter value) to the distribution induced by the approximation gives an indication of whether or not the approximation can adequately represent the MJP. By using efficient space filling designs to explore the parameter space, we can assess an approximate simulator across a large region. In particular, since each point in the Latin hypercube design can be simulated independently, we can use cloud computing to explore vast regions of the parameter space.

We applied our approach to three examples in which the underlying Markov jump process exhibits interesting non-linear dynamics. For the Schlögl system (Section 4.1), our approach was able to detect a region of bi-modality using relatively few design points. In the Lotka-Volterra example (Section 4.2), a comparison of the linear noise approximation and moment closure approach was able to identify regions of the parameter space that lead to prey extinction. Finally, for the prokaryotic auto regulatory gene network (Section 4.3), we considered the synthetic data set of Milner et al. [2013] and compared the moment closure approach with the MJP over parameter regions determined both *a priori* and *a posteriori*. We found that in regions of high posterior density, the approximation does appear to provide a satisfactory alternative to the MJP, despite the inherent discreteness of the observed data.

Computing details

All simulations were performed on a machine with 16GB of RAM and with an Intel quad-core CPU. The operating system used was Ubuntu 12.04. Simulations for the Lotka-Volterra model and Schlögl system were performed using R (version 3.3.1), via the `issb` package (version 0.13.3) (R Core Team and R Development Core Team [2013], Golightly and Gillespie [2013]. The Latin hypercube was generated using the `lhs` package (version 0.13) [Carnell, 2012]. The graphics were created using the `ggplot2` R package (version 2.1.0) [Wickham, 2009]. The Prokaryotic auto regulatory gene network code used a combination of C (from the Milner et al. [2013] paper) and R code.

Acknowledgements: We thank the three anonymous referees for constructive comments that have improved the paper.

References

L. S. Bastos and A. O'Hagan. Diagnostics for Gaussian Process Emulators. *Technometrics*, 51(4):425–438, Nov. 2009. ISSN 0040-1706. doi: 10.1198/TECH.2009.08019.

M. A. Beaumont, W. Zhang, and D. J. Balding. Approximate Bayesian Computation in Population Genetics. *Genetics*, 162(4):2025–2035, 2002.

R. J. Boys, D. J. Wilkinson, and T. B. L. Kirkwood. Bayesian inference for a discretely observed stochastic kinetic model. *Statistics and Computing*, 18(2):125–135, 2008. ISSN 0960-3174. doi: 10.1007/s11222-007-9043-x.

Y. Cao and L. R. Petzold. Accuracy limitations and the measurement of errors in the stochastic simulation of chemically reacting systems. *Journal of Computational Physics*, 212(1):6–24, Feb. 2006. ISSN 00219991. doi: 10.1016/j.jcp.2005.06.012.

Y. Cao, H. Li, and L. R. Petzold. Efficient formulation of the stochastic simulation algorithm for chemically reacting systems. *The Journal of Chemical Physics*, 121(9): 4059–67, Sept. 2004. ISSN 0021-9606. doi: 10.1063/1.1778376.

R. Carnell. *lhs: Latin Hypercube Samples*, 2012. URL http://cran.r-project.org/package=lhs.

J. Elf and M. Ehrenberg. Fast evolution of fluctuations in biochemical networks with the linear noise approximation. *Genome Res.*, 13(11):2475–2484, 2003.

C. W. Gardiner. *Handbook of stochastic methods for physics, chemistry, and the natural sciences*, volume 13 of *Springer series in synergetics*. Springer-Verlag, Berlin Heidelberg New York, 2 edition, 1985.

M. A. Gibson and J. Bruck. Efficient Exact Stochastic Simulation of Chemical Systems with Many Species and Many Channels. *The Journal of Physical Chemistry A*, 104 (9):1876–1889, Mar. 2000. ISSN 1089-5639. doi: 10.1021/jp993732q.

C. S. Gillespie. Moment-closure approximations for mass-action models. *IET Systems Biology*, 3(1):52–8, 2009. ISSN 1751-8849. doi: 10.1049/iet-syb:20070031.

D. T. Gillespie. A general method for numerically simulating the stochastic time evolution of coupled chemical reactions. *Journal of Computational Physics*, 22(4): 403–434, Dec. 1976. ISSN 00219991. doi: 10.1016/0021-9991(76)90041-3.

D. T. Gillespie. A rigorous derivation of the chemical master equation. *Physica A: Statistical Mechanics and its Applications*, 188(1-3):404–425, Sept. 1992. ISSN 03784371. doi: 10.1016/0378-4371(92)90283-V.

D. T. Gillespie. The chemical Langevin equation. *The Journal of Chemical Physics*, 113 (1):297–306, 2000.

A. Golightly and C. S. Gillespie. Simulation of stochastic kinetic models. In M. V. Schneider, editor, *Methods in Molecular Biology*, volume 1021, pages 169–87. Humana Press, Jan. 2013. doi: 10.1007/978-1-62703-450-0_9.

A. Golightly and D. J. Wilkinson. Bayesian inference for nonlinear multivariate diffusion models observed with error. *Computational Statistics & Data Analysis*, 52(3):1674–1693, Jan. 2008. ISSN 01679473. doi: 10.1016/j.csda.2007.05.019.

A. Golightly and D. J. Wilkinson. Bayesian parameter inference for stochastic biochemical network models using particle MCMC. *Interface Focus*, pages 807–820, 2011.

A. Golightly, D. A. Henderson, and C. Sherlock. Delayed acceptance particle MCMC for exact inference in stochastic kinetic models. *Statistics and Computing*, May 2015. ISSN 09603174. doi: 10.1007/s11222-014-9469-x.

R. Grima. A study of the accuracy of moment-closure approximations for stochastic chemical kinetics. *The Journal of Chemical Physics*, 136(15):154105, Apr. 2012. ISSN 1089-7690. doi: 10.1063/1.3702848.

B. Ingalls. Sensitivity analysis: from model parameters to system behaviour. In O. Wolkenhauer, P. Wellstead, and C. Kwang-Hyun, editors, *Essays in Biochemistry - Systems Biology*, pages 177–193. Portland Press, London, 2008.

G. Jenkinson and J. Goutsias. Statistically testing the validity of analytical and computational approximations to the chemical master equation. *The Journal of Chemical Physics*, 138(20):204108, 2013a. ISSN 1089-7690. doi: 10.1063/1.4807390.

G. Jenkinson and J. Goutsias. Statistical validation of parametric approximations to the master equation. In *2013 Asilomar Conference on Signals, Systems and Computers*, pages 1721–1725. IEEE, Nov. 2013b. ISBN 978-1-4799-2390-8. doi: 10.1109/ACSSC.2013.6810595.

A. Kowald and T. Kirkwood. A network theory of ageing: the interactions of defective mitochondria, aberrant proteins, free radicals and scavengers in the ageing process. *Mutation Research/DNAging*, 316(5-6):209–236, May 1996. ISSN 09218734. doi: 10.1016/S0921-8734(96)90005-3.

T. G. Kurtz. Solutions of ordinary differential equations as limits of pure jump markov processes. *J. Appl. Probab..*, 7:49–58, 1970.

A. J. Lotka. *Elements of Physical Biology*. Baltimore: Williams and Wilkins, 1925.

J. M. McCollum, G. D. Peterson, C. D. Cox, M. L. Simpson, and N. F. Samatova. The sorting direct method for stochastic simulation of biochemical systems with varying reaction execution behavior. *Computational Biology and Chemistry*, 30(1):39–49, Feb. 2006. ISSN 1476-9271. doi: 10.1016/j.compbiolchem.2005.10.007.

M. D. McKay, R. J. Beckman, and W. J. Conover. Comparison of Three Methods for Selecting Values of Input Variables in the Analysis of Output from a Computer Code. *Technometrics*, 21(2):239–245, May 1979. ISSN 0040-1706. doi: 10.1080/00401706.1979.10489755.

P. Milner, C. S. Gillespie, and D. J. Wilkinson. Moment closure based parameter inference of stochastic kinetic models. *Statistics and Computing*, 23(2):287–295, Jan. 2013. ISSN 09603174. doi: 10.1007/s11222-011-9310-8.

M. D. Morris and T. J. Mitchell. Exploratory designs for computational experiments. *Journal of Statistical Planning and Inference*, 43(3):381–402, Feb. 1995. ISSN 03783758. doi: 10.1016/0378-3758(94)00035-T.

M. Opper and G. Sanguinetti. Variational inference for Markov jump processes. In J. C. Platt, D. Koller, Y. Singer, and S. T. Roweis, editors, *Advances in Neural Information Processing Systems 20*, pages 1105–1112. Curran Associates, Inc., 2008.

J. Owen, D. J. Wilkinson, and C. S. Gillespie. Likelihood free inference for Markov processes: a comparison. *Statistical Applications in Genetics and Molecular Biology*, 14(2):189–209, 2015.

J. Pahle. Biochemical simulations: stochastic, approximate stochastic and hybrid approaches. *Briefings in Bioinformatics*, 10(1):53–64, Jan. 2009. ISSN 1477-4054. doi: 10.1093/bib/bbn050.

R Core Team and R Development Core Team. R: A Language and Environment for Statistical Computing, 2013. URL http://www.r-project.org.

H. Salis and Y. Kaznessis. Accurate hybrid stochastic simulation of a system of coupled chemical or biochemical reactions. *The Journal of Chemical Physics*, 122(5):54103, Feb. 2005. ISSN 0021-9606. doi: 10.1063/1.1835951.

D. Schnoerr, G. Sanguinetti, and R. Grima. Validity conditions for moment closure approximations in stochastic chemical kinetics. *The Journal of Chemical Physics*, 141 (8):084103, Aug. 2014. ISSN 0021-9606. doi: 10.1063/1.4892838.

C. Sherlock, A. Golightly, and C. S. Gillespie. Bayesian inference for hybrid discrete-continuous systems biology models. *Inverse Problems*, 30:114005, 2014.

A. Singh and J. P. Hespanha. A derivative matching approach to moment closure for the stochastic logistic model. *Bulletin of Mathematical Biology*, 69:1909–1925, 2007.

S. A. Sisson, Y. Fan, and M. M. Tanaka. Sequential Monte Carlo without likelihoods. *Proceedings of the National Academy of Sciences*, 104(6):1760–1765, 2007. doi: 10.1073/pnas.0607208104.

P. Smadbeck and Y. N. Kaznessis. A closure scheme for chemical master equations. *Proceedings of the National Academy of Sciences*, 110:14261–14265, 2013.

T. Toni, D. Welch, N. Strelkowa, A. Ipsen, and M. P. H. Stumpf. Approximate Bayesian computation scheme for parameter inference and model selection in dynamical systems. *Journal of The Royal Society Interface*, 6(31):187–202, Feb. 2009. doi: 10.1098/rsif.2008.0172.

N. G. van Kampen. *Stochastic Processes in Physics and Chemistry*. North Holland, 3 edition, 2007.

V. Volterra. Fluctuations in the abundance of a species considered mathematically. *Nature*, 118:558–660, 1926.

S. R. White, T. Kypraios, and S. P. Preston. Piecewise Approximate Bayesian Computation: fast inference for discretely observed Markov models using a factorised posterior distribution. *Statistics and Computing*, Nov. 2013. ISSN 0960-3174. doi: 10.1007/s11222-013-9432-2.

H. Wickham. *ggplot2: Elegant Graphics for Data Analysis*. Springer, New York, 2009. ISBN 978-0-387-98140-6.

D. J. Wilkinson. *Stochastic Modelling for Systems Biology*. Chapman & Hall/CRC, London, 2nd edition, 2012.